THE JOURNAL OF BIOLOGICAL CHEMISTRY
Vol. 277, No. 8, Issue of February 22, pp. 6111–6117, 2002

Printed in U.S.A.

Human Cationic Trypsinogen

Arg^{117} IS THE REACTIVE SITE OF AN INHIBITORY SURFACE LOOP THAT CONTROLS SPONTANEOUS ZYMOGEN ACTIVATION*

Received for publication, September 15, 2001, and in revised form, December 14, 2001
Published, JBC Papers in Press, December 17, 2001, DOI 10.1074/jbc.M110959200

Zoltán Kukor, Miklós Tóth‡, Gábor Pál§, and Miklós Sahin-Tóth¶

From the Department of Physiology, University of California Los Angeles, Los Angeles, California 90095-1662

Mutation of Arg^{117}, an autocatalytic cleavage site, is the most frequent amino acid change found in the cationic trypsinogen (Tg) of patients with hereditary pancreatitis. In the present study, the role of Arg^{117} was investigated in wild-type cationic Tg and in the activation-resistant $Lys^{15} \rightarrow Gln$ mutant (K15Q-Tg), in which Tg-specific properties of Arg^{117} can be examined selectively. We found that trypsinolytic cleavage of the Arg^{117}-Val^{118} bond did not proceed to completion, but due to trypsin-catalyzed re-synthesis an equilibrium was established between intact Tg and its cleaved, two-chain form. In the absence of Ca^{2+}, at pH 8.0, the hydrolysis equilibrium (K_{hyd} = [cleaved Tg]/[intact Tg]) was 5.4, whereas 5 mM Ca^{2+} reduced the *rate* of cleavage at Arg^{117} at least 20-fold, and shifted K_{hyd} to 0.7. These observations indicate that the Arg^{117}-Val^{118} bond exhibits properties analogous to the reactive site bond of canonical trypsin inhibitors and suggest that this surface loop might serve as a low affinity inhibitor of zymogen activation. Consistent with this notion, autoactivation of cationic Tg was inhibited by the cleaved form of K15Q-Tg, with an estimated K_i of 80 μM, while no inhibition was observed with K15Q-Tg carrying the $Arg^{117} \rightarrow$ His mutation. Finally, zymogen breakdown due to other trypsinolytic pathways was shown to proceed almost 2000-fold slower than cleavage at Arg^{117}. Taken together, the findings suggest two independent, successively functional trypsin-mediated mechanisms against pathological Tg activation in the pancreas. At low trypsin concentrations, cleavage at Arg^{117} results in inhibition of trypsin, whereas high trypsin concentrations degrade Tg, thus limiting further zymogen activation. Loss of Arg^{117}-dependent trypsin inhibition can contribute to the development of hereditary pancreatitis associated with the $Arg^{117} \rightarrow$ His mutation.

Autosomal-dominant hereditary pancreatitis (HP)[1] is associated with several mutations in the *PRSS1* gene encoding human cationic trypsinogen (Tg). According to a recent report from the Midwest Multicenter Pancreatic Study Group (1), the great majority (76%) of Tg mutations affects the Arg^{117} residue in the Tg sequence (chymotrypsin numbering), changing it to either His (R117H, 75% (2)) or rarely to Cys (R117C, 1% (3–5)). The second most frequent target of HP mutations is Asn^{21}, where mutations $Asn^{21} \rightarrow$ Ile (N21I, 20% (6–8)) and $Asn^{21} \rightarrow$ Thr (N21T, 1% (5)) have been identified so far. In addition, several other rare Tg mutations have been described in patients with HP or other forms of chronic pancreatitis (8–14).

The discovery of HP mutations provided strong support that Tg and/or trypsin (Tr) plays a central role in the pathogenesis of human pancreatitis. Although the precise mechanisms leading to pancreatitis have not been unraveled, increased Tr activity in the pancreas due to altered properties of mutant Tg/Tr emerged as a generally accepted model. Consequently, the biochemical defects, gain or loss of function, caused by mutations of Arg^{117} and Asn^{21} have been the target of intense research in recent years. Early studies used recombinant rat anionic Tg as a model for human cationic Tg (15–18), but, lately, techniques have been developed that allowed recombinant expression and *in vitro* refolding of the human enzyme (19–22). Experiments using these recombinant cationic Tg preparations have addressed four major aspects of Tg/Tr biochemistry, with the following developments: (i) Autocatalytic degradation (autolysis) of Tr was inhibited by mutations R117H (20, 21), R117C (3), and N21T (19), whereas mutation N21I (19–22) had no such effect. (ii) Autocatalytic activation (autoactivation) of Tg was enhanced by all four mutations (N21T, N21I, R117H, R117C) studied so far (3, 19–22). Interestingly, increased autoactivation of N21I was prominent only at pH 5.0. A study using model peptides corresponding to the N terminus of Tg suggested that the rare K15R and D14G mutations might also increase Tg autoactivation (12), however, supporting data on recombinant enzymes are still lacking. (iii) Cathepsin B, a lysosomal cysteine protease, is believed to be responsible for initiating zymogen activation in animal models of experimental pancreatitis (see Ref. 23, and references therein). It was reported (22) that the N21I cationic Tg mutant was activated almost 3-fold faster by cathepsin B than wild-type Tg, even in the presence of pancreatic secretory Tr inhibitor (PSTI). However, these observations could not be independently confirmed, because in more recent experiments mutants N21I, R117H, R117C and wild-type Tg exhibited no appreciable differences in activation by cathepsin B (3).[2] (iv) The ability of PSTI to inhibit the N21I Tr mutant was also investigated, but no difference was found when compared with wild-type Tr (22). Taken together, the bulk of evidence suggests that increased autoactivation is a common mechanism by which HP-associated muta-

* This work was supported by National Institutes of Health Grant DK58088. The costs of publication of this article were defrayed in part by the payment of page charges. This article must therefore be hereby marked "*advertisement*" in accordance with 18 U.S.C. Section 1734 solely to indicate this fact.

‡ Present address: Dept. of Medical Chemistry, Molecular Biology and Pathobiochemistry, Semmelweis University, Budapest, Puskin utca 9, 1088, Hungary.

§ Present address: Dept. of Biochemistry and Molecular Biology, University of Chicago, 920. E. 58th St., Chicago, IL 60637.

¶ To whom correspondence should be addressed: HHMI/UCLA, 5-748 MacDonald Research Laboratories, Box 951662, Los Angeles, CA 90095-1662. Tel.: 310-206-5055; Fax: 310-206-8623; E-mail: miklos@hhmi.ucla.edu.

[1] The abbreviations used are: HP, hereditary pancreatitis; Tg, trypsinogen; Tr, trypsin; Tg*, two-chain trypsinogen with the Arg^{117}-Val^{118} peptide bond cleaved; Tr*, two-chain trypsin with the Arg^{117}-Val^{118} peptide bond cleaved; PSTI, pancreatic secretory trypsin inhibitor.

[2] Z. Kukor, M. Tóth, and M. Sahin-Tóth, unpublished observations.

tions can lead to pathological Tr accumulation in the pancreas. In addition, Tr stabilization appears to be an accessory pathway, associated with mutations R117H, R117C, and N21T. Although it is now generally accepted that HP mutations lead to a gain of function, a recent report (3) challenged this notion by demonstrating that almost 70% of mutant R117C was misfolded and inactive after recombinant expression and *in vitro* refolding. It remains unclear, however, whether or not the same folding defect is manifested *in vivo*. In any event, the correctly folded fraction of the R117C mutant exhibited gain-of-function properties that were similar to those of the R117H mutant.

Despite considerable progress in the field, the mechanism(s) by which the mutations cause the described functional changes are still unclear. In the present study, we set out to investigate the role Arg^{117} might play in Tg activation and how mutations in Arg^{117} can enhance zymogen activation. Unexpectedly, we found that Tr not only cleaved the Arg^{117}-Val^{118} bond but also re-synthesized it until an equilibrium was reached between the cleaved and intact Tg forms. These properties of Arg^{117} resemble the reactive site of reversible canonical protease inhibitors (24) and suggest that Arg^{117} plays an inhibitory role in controlling zymogen activation in the pancreas. Evidence to support this notion is presented here, and a model describing the dual role of Tr in protecting against pathological Tg activation is discussed.

EXPERIMENTAL PROCEDURES

Nomenclature—In this article the classic chymotrypsin numbering was used to denote amino acid residues in the human cationic Tg sequence. In more recent genetic and clinical literature the actual Tg sequence numbering has been used by convention (25). In the chymotrypsin numbering system Asp^{14}, Lys^{15}, Asn^{21}, Arg^{117}, Val^{118}, Lys^{188}, and Asp^{189} correspond to Tg residues Asp^{22}, Lys^{23}, Asn^{29}, Arg^{122}, Val^{123}, Lys^{193}, and Asp^{194}, respectively. Following the designation of cleaved canonical protease inhibitors (24), the two-chain autolyzed form of Tg with the Arg^{117}-Val^{118} bond cleaved was denoted here as Tg*. In previous studies bovine Tg and Tr, autolyzed at the Arg^{117}-Val^{118} bond, were also named Val-neotrypsinogen (26) or δ-trypsin (27), respectively.

Mutagenesis—Mutant K15Q was constructed in the previously described pTrap-T7 expression plasmid (19). A synthetic oligonucleotide linker encoding the mutation was ligated into the *Nco*I and *Eco*RI sites. Mutant K15Q/R117H was created by subcloning the *Eco*RI-*Sac*I fragment from the pTrap-T7/R117H plasmid (20) into the pTrap-T7/K15Q plasmid.

Expression and Purification of Tg—Small scale expression of Tg was carried out essentially as previously reported (19–21). For larger scale expression, 800-ml cultures of Rosetta(DE3) (Novagen) cells harboring pTrap-T7 with given Tg constructs were grown in Luria-Bertani medium with 50 μg/ml carbenicillin and 34 μg/ml chloramphenicol to an $A_{600\ nm}$ of 0.5, induced with 1 mM isopropyl 1-thio-β-D-galactopyranoside, and grown for an additional 5 h. Rosetta(DE3) host strains are BL21(DE3) derivatives designed to enhance the expression of eukaryotic proteins that contain codons rarely used in *Escherichia coli*. Cells were harvested by centrifugation, resuspended in 60 ml of 0.1 M Tris-HCl (pH 8.0), 5 mM K-EDTA, and disrupted by one passage through a French press cell at 25,000 p.s.i. Inclusion bodies were pelleted by centrifugation and washed twice with 25 ml of 0.1 M Tris-HCl (pH 8.0), 5 mM EDTA. Solubilization and *in vitro* refolding of Tg was performed as described previously (19, 22) in 0.9 M guanidine-HCl, 0.1 M Tris-HCl (pH 8.0) containing 1 mM L-cystine and 1 mM L-cysteine. The properly folded Tg was finally purified on an ecotin affinity column, as described (18–20). Concentrations of zymogen solutions were measured from their ultraviolet absorbance using a calculated extinction coefficient of 36,160 M^{-1} cm^{-1} at 280 nm. Tg yields were lower than previously reported (19), typically 2–4 mg of purified zymogen per liter culture.

*Isolation of Tg**—Wild-type Tg was allowed to autoactivate in 1 mM EDTA, 0.1 M Tris-HCl (pH 8.0), at 37 °C for 2 h. K15Q-Tg was digested with cationic Tr at a ratio of ~1:250 Tr to K15Q-Tg in 1 mM EDTA, 0.1 M Tris-HCl (pH 8.0), at 37 °C for 20 min. Samples were immediately loaded onto a MonoQ HR 5/5 column (Amersham Biosciences, Inc.) equilibrated with 20 mM Tris-HCl (pH 8.8). Tg and Tg* were eluted and separated from each other with 25 ml of a 0–0.5 M linear gradient of NaCl. Under these conditions Tr did not bind to the column and was recovered in the flow-through. Fractions (0.5 ml) containing Tg* or K15Q-Tg* were pooled and dialyzed against 1 mM HCl overnight.

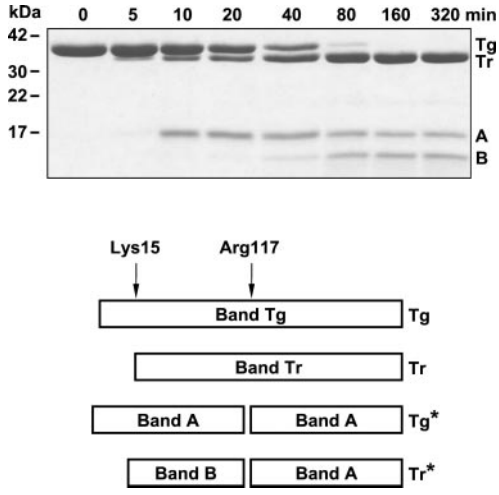

FIG. 1. **Activation of human cationic Tg with Tr.** Approximately 3 μM wild-type Tg (final concentration) was incubated with 0.3 μM human cationic Tr (final concentration) at 37 °C, in 0.1 M Tris-HCl (pH 8.0) and 5 mM $CaCl_2$ in a final volume of 100 μl. Reactions were terminated at the indicated times by precipitation with trichloroacetic acid, electrophoresed on 12% gels under reducing conditions, and stained with Coomassie Blue. The *0 min* control lane contains no Tr. *Tg*, trypsinogen; *Tr*, trypsin; *A* and *B*, proteolytic fragments; see text for details. The *cartoon* indicates the positions of the Lys^{15} and Arg^{117} trypsinolytic sites in Tg and the fragments generated by their cleavage. Note that the two fragments present in *band A* are held together by a disulfide bond in Tg* and they only separate in the reducing sample buffer used for electrophoresis.

Autoactivation of Tg—Human cationic Tg (2 μM final concentration in 100-μl final volume) was incubated at 37 °C in 0.1 M Tris-HCl (pH 8.0) or 0.1 M sodium acetate buffer (pH 5.0), in the presence of 5 mM $CaCl_2$ where indicated. At given times 2.5-μl aliquots were removed for Tr activity assays. Tr activity was determined using the synthetic chromogenic substrate *N*-carbobenzyloxy-Gly-Pro-Arg-*p*-nitroanilide (200 μM final concentration). Kinetics of the chromophore release was followed at 405 nm in 0.1 M Tris-HCl (pH 8.0), 1 mM $CaCl_2$, at 22 °C.

Gel Electrophoresis and Densitometric Analyses—Where indicated, samples were precipitated with trichloroacetic acid (10% final concentration), incubated on ice for 10 min, and centrifuged for 10 min at 14,000 rpm in an Eppendorf bench top centrifuge at 4 °C. Laemmli sample buffer (20 μl), NaOH (1 μl, 2 N), and dithiothreitol (2 μl, 1 M) were added, and samples were denatured at 90 °C for 5 min. Electrophoretic separation was performed on 12% SDS-PAGE gels. Gels were stained with Coomassie Brilliant Blue R for 30 min and destained with 30% methanol, 10% acetic acid overnight. Gels were dried between two layers of cellophane according to instructions of the Gel-Dry (Invitrogen) gel drying kit. Dried gels were scanned at 600 d.p.i. resolution in gray-scale mode, and images were saved as TIFF files. Quantitation of gel bands was carried out with the ImageQuaNT 5.2 (Molecular Dynamics) software. Rectangles were drawn around each band of interest, and an identical rectangle was used in each lane for background subtraction.

RESULTS

Cleavage of the Arg^{117}-Val^{118} Peptide Bond Occurs during Tg Activation—The *gel image* in Fig. 1 demonstrates the time course of activation of Tg with Tr, in 5 mM Ca^{2+} at pH 8.0, 37 °C. Conversion of Tg to Tr upon cleavage after Lys^{15} is indicated by a mobility shift on 12% SDS-PAGE gels (band Tg → band Tr), because Tr migrates faster than Tg under these electrophoretic conditions. In addition to activation, Tr cleaves Tg also at the Arg^{117}-Val^{118} autolytic peptide bond, resulting in the appearance of band A on reducing gels. As we demonstrated previously (19), band A corresponds to a mixture of two co-migrating polypeptides with nearly identical sizes, namely the N- and C-terminal fragments of autolyzed Tg. This two-

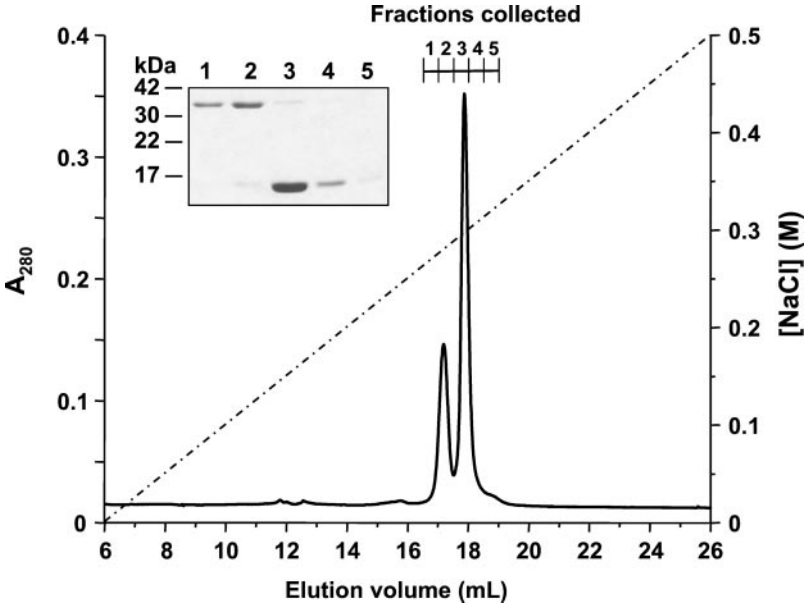

FIG. 2. **Chromatographic separation of intact and Arg^{117}-cleaved forms of wild-type Tg.** In the representative experiment presented here, ~5 μM wild-type Tg (final concentration) was incubated at 37 °C, in 0.1 M Tris-HCl (pH 8.0) and 1 mM K-EDTA for 2 h in a final volume of 5 ml. The reaction mixture was then loaded onto a MonoQ HR 5/5 column (Amersham Biosciences, Inc.) equilibrated with 20 mM Tris-HCl (pH 8.8), and protein was eluted with a linear 0–0.5 M NaCl gradient (*right axis*). Fractions (0.5 ml) were collected where indicated, and 20 μl was directly analyzed on a 12% reducing SDS-PAGE gel (*inset*).

chain form of Tg with the Arg^{117}-Val^{118} bond cleaved will be referred to as Tg* in this report. Tg* is also activated by Tr, which is evidenced by the appearance of *band B* on reducing gels. *Band B* is generated from *band A* by removal of the activation peptide from the N-terminal Tg* fragment. Thus, *band B* corresponds to the N-terminal fragment of two-chain, Arg^{117}-cleaved Tr (Tr*). Note that the two chains in Tg* and Tr* are held together by a disulfide bond and they only separate under the reducing conditions used for SDS-PAGE gel analysis.

*Isolation of Two-chain Tg**—We observed that Tr-catalyzed activation of Tg* seemed to proceed slower than Tr-catalyzed activation of intact Tg. Thus, *band B* always emerged later in the time course and was noticeably lighter in intensity than the *Tr band* (Fig. 1). This observation led to the hypothesis that cleavage of Tg at Arg^{117} hinders Tg activation, as we first believed due to a conformational change in the Tg structure. To test this assumption, we isolated Tg* using anion-exchange chromatography, and compared its activation properties to intact wild-type Tg. Tg* was generated from wild-type Tg by limited autoactivation of Tg in the absence of Ca^{2+}. As we demonstrated previously (19), under these conditions Tg is cleaved predominantly after Arg^{117}, whereas cleavage after Lys^{15} is suppressed. Thus, the major product is Tg* and only small amounts of Tr are generated. Tg* was then separated on a MonoQ column at alkaline pH, where it eluted after the intact Tg peak (Fig. 2). The *gel inset* indicates the purity of these preparations, which was greater than >95%, with small amounts of intact Tg present.

Unexpected Re-synthesis of the Arg^{117}-Val^{118} Bond—Although data are not shown, when the activation process was followed by measuring Tr activity, we did not observe any appreciable differences between the activation characteristics of intact Tg and Tg*. Enterokinase or Tr activated both Tg forms at comparable rates, and Ca^{2+} dependence of autoactivation was indistinguishable. These observations did not support our original hypothesis and indicated that cleavage of Tg at Arg^{117} had no direct effect on Tg activation. Furthermore, enzyme kinetic parameters of Tr and Tr* were essentially identical, in agreement with previous reports that cleavage of the Arg^{117}-Val^{118} bond in bovine (28) or porcine (29) Tr has no obvious functional consequences. However, when the time course of autoactivation was followed on SDS-PAGE gels an unexpected observation was made. As shown in Fig. 3*A*, at pH 8.0, in 5 mM Ca^{2+}, the majority of Tg* was converted back to intact Tg and activated to intact Tr. Attempts to extend these observations revealed that experiments with wild-type Tg and Tr were difficult to interpret quantitatively. Due to the continuous conversion of Tg to Tr, concentrations of substrate (Tg) and enzyme (Tr) were constantly changing during the reaction. In addition, Tr can cleave the Arg^{117}-Val^{118} bond not only in Tg but also in Tr. This latter process is also reversible due to the re-synthesis of the Arg^{117}-Val^{118} bond in Tr* (not shown). In the present study we focused selectively on the interaction of Tr with Tg, and the role of Arg^{117} in Tg. Similar experiments on the properties of Arg^{117} in Tr will be presented elsewhere.

To gain deeper insight into the extraordinary phenomenon of Tr-catalyzed re-synthesis of Tg*, an activation-resistant Tg mutant was constructed, where Lys^{15} in the activation peptide was mutated to Gln (K15Q-Tg). In this zymogen, Arg^{117} is the only readily accessible trypsinolytic site, and thus its properties can be selectively studied. A two-chain form of K15Q-Tg cleaved between Arg^{117} and Val^{118} (K15Q-Tg*) was also isolated, as described above. When this Tg preparation was treated with cationic Tr, time-dependent re-synthesis of the intact single-chain form was evident, without any significant degradation (Fig. 3*B*). No re-synthesis was observed in the absence of Tr or with the catalytically incompetent S195A Tr mutant. As shown in Fig. 3*C*, the re-synthesis did not proceed to completion, but an apparent equilibrium was reached between intact Tg and Tg* with a hydrolysis equilibrium of 0.73 (K_{hyd} = [Tg*]/[Tg]), corresponding to a ratio of ~40% Tg* to 60% Tg.

Trypsinolysis of the Arg^{117}-Val^{118} Bond Is Self-limiting—When intact K15Q-Tg was digested with catalytic amounts (~1:160 ratio) of cationic Tr in the absence of Ca^{2+} at pH 8.0, rapid cleavage at Arg^{117} was evident (Fig. 4*A*). Surprisingly, digestion remained incomplete over the entire time course, as a stable equilibrium was reached between the predominant cleaved form (~85%) and the remaining intact K15Q-Tg (~15%), yielding a K_{hyd} of 5.4. Increasing concentrations of Ca^{2+} reduced the *rate* of cleavage at Arg^{117} significantly. Estimation of the relative rates by comparing the initial segments of digestion kinetics obtained in the absence of Ca^{2+} (Fig. 4*A*) or in 5 mM Ca^{2+} (Fig. 4*D*) indicated an at least 20-fold decrease (Fig. 4*E*). In addition, Ca^{2+} also lowered the K_{hyd} values from 5.4 to 0.96 and 0.7 in 0.1 mM Ca^{2+} (Fig. 4*B*) and 0.5 mM Ca^{2+} (Fig. 4*C*), respectively. It is also apparent from Fig. 4*E* that in

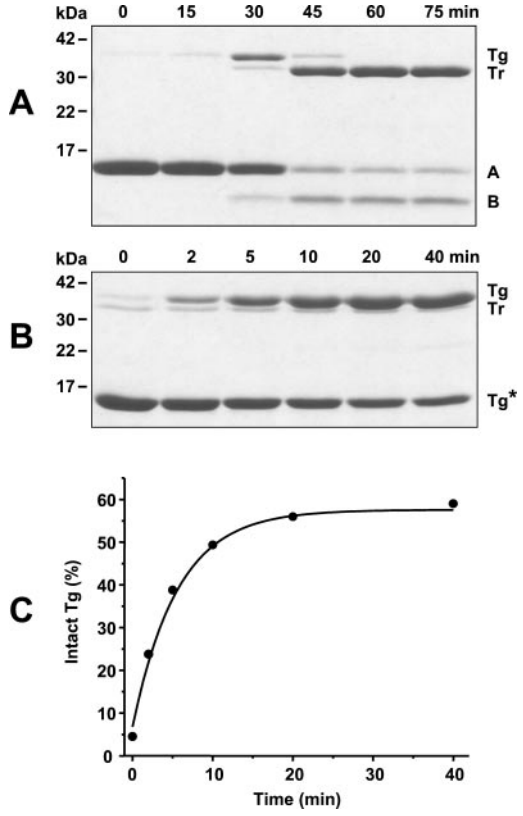

FIG. 3. **Re-synthesis of the Arg^{117}-Val^{118} peptide bond in wild-type Tg and K15Q-Tg.** Reactions were carried out at 37 °C, in 0.1 M Tris-HCl (pH 8.0) and 5 mM $CaCl_2$. *A*, 2.8 μM purified Tg* (final concentration) was incubated. *B*, 4 μM purified K15Q-Tg* was incubated with 0.3 μM cationic Tr (final concentrations). Reactions were terminated at indicated times by precipitation with trichloroacetic acid, electrophoresed on 12% gels, and stained with Coomassie Blue. *C*, densitometric quantitation of *B*. The intensity of the Tg band was expressed as percentage of total density, *i.e.* the sum of bands Tg and Tg*.

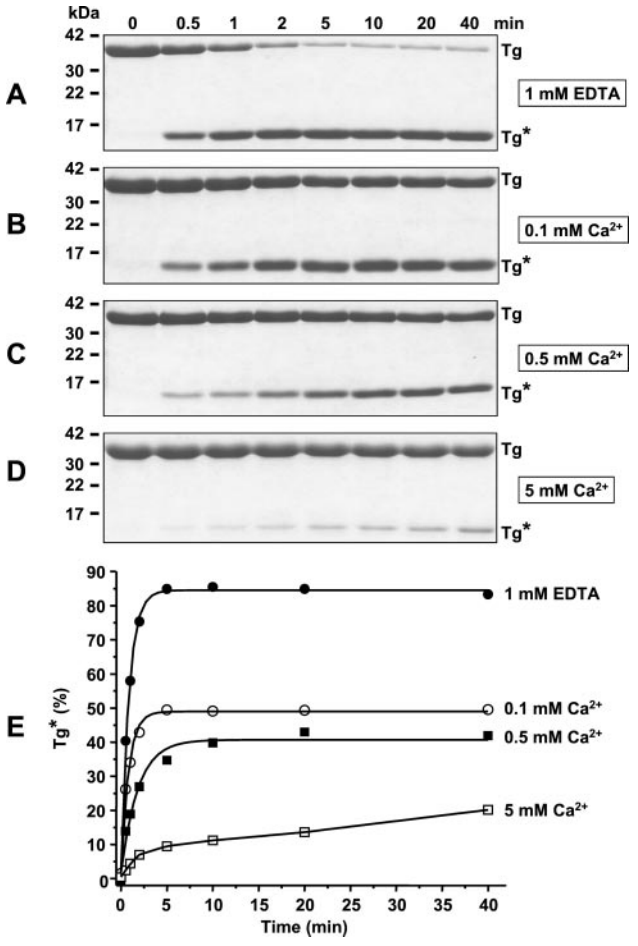

FIG. 4. **Effect of Ca^{2+} on the digestion of the Arg^{117}-Val^{118} bond in K15Q-Tg with cationic Tr.** Aliquots (5 μM, final concentration) of K15Q-Tg were digested with 30 nM cationic Tr (final concentration) at 37 °C, in 0.1 M Tris-HCl (pH 8.0), and in 1 mM K-EDTA or the indicated concentrations of $CaCl_2$. *A–D*, reactions were terminated at indicated times by trichloroacetic acid precipitation and analyzed by reducing SDS-PAGE and Coomassie Blue staining. Note that the low amounts of Tr used for digestion were not visible on the gels. *E*, densitometric quantitation of gels in *A–D*. The intensity of *band Tg** was expressed as percentage of total density, *i.e.* the sum of *bands Tg* and *Tg**.

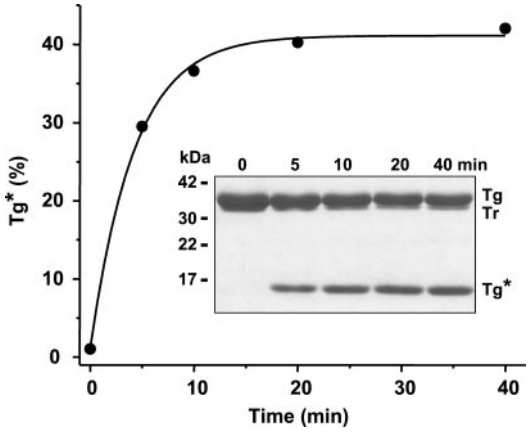

FIG. 5. **Digestion of the Arg^{117}-Val^{118} bond in K15Q-Tg in 5 mM Ca^{2+}.** The experiment was carried out as described in Fig. 4, except that 0.5 μM cationic Tr (final concentration) was used.

5 mM Ca^{2+} an equilibrium was not reached during the time course studied. When digestions in 5 mM Ca^{2+} were carried out with higher Tr concentrations (Fig. 5), an equilibrium could be demonstrated with a K_{hyd} of 0.7, a value that was essentially identical with that observed in the re-synthesis experiments in Fig. 3. It is noteworthy that the K_{hyd} value remained constant when concentrations of Ca^{2+} were increased from 0.5 to 5 mM, although the rate of cleavage at Arg^{117} was further depressed, and the same equilibrium state was reached much slower. It must also be emphasized that in these experiments Tr behaved only as a catalyst facilitating the development of the hydrolysis equilibrium between the intact and Arg^{117}-cleaved forms of K15Q-Tg. Consequently, given sufficient time, similar equilibrium states were reached regardless of the Tr concentration present in the incubation mixtures (data not shown).

Arg^{117} Is the Reactive Site of a Weakly Inhibitory Loop—The observations described above indicate that the Arg^{117}-Val^{118} bond in cationic Tg exhibits properties that are in many respects analogous to those of reversible canonical Tr inhibitors (Ref. 24, and references therein). Thus, (i) Arg^{117} is a "hyper-exposed" Arg on a surface loop of Tg, (ii) cleavage of this bond leads to an equilibrium between the intact and cleaved forms, and (iii) the same equilibrium can be demonstrated through Tr-catalyzed re-synthesis of the cleaved species. Taken together, these characteristics suggest that Arg^{117} might be the reactive site of an inhibitory loop in Tg. One significant difference from canonical protease inhibitors is the fast rate of hydrolysis, which suggests that inhibitory properties of Arg^{117} are likely to be relatively weak (30). To test this hypothesis, we examined the effect of high concentrations (80 μM) of the non-activable K15Q-Tg and K15Q-Tg* on the autoactivation of wild-type cationic Tg. In control samples, instead of K15Q-Tg

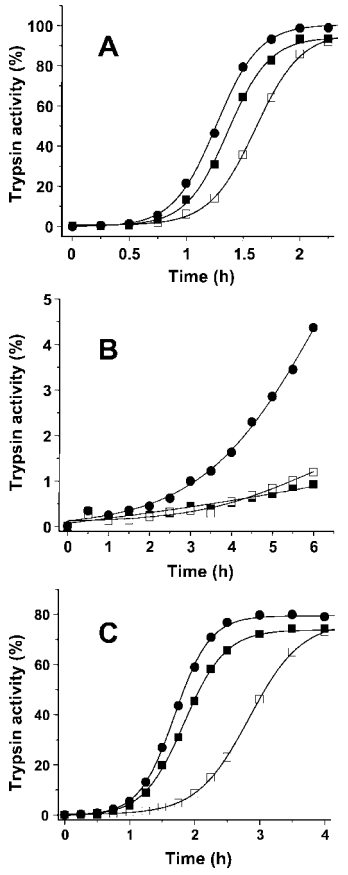

FIG. 6. **Effect of K15Q-Tg and K15Q-Tg* on the autoactivation of wild-type Tg.** Approximately 2 μM wild-type Tg was incubated at 37 °C, with 80 μM (final concentrations) K15Q-Tg (■) or K15Q-Tg* (□). In control samples, 80 μM K15Q/R117H-Tg (●) was included. Reactions were carried out in (*A*) 0.1 M Tris-HCl (pH 8.0), 5 mM $CaCl_2$, (*B*) 0.1 M Tris-HCl (pH 8.0) with no Ca^{2+} added, or (*C*) in 0.1 M sodium acetate buffer (pH 5.0), 5 mM $CaCl_2$, in a final volume of 100 μl. Aliquots of 2.5 μl were withdrawn from reaction mixtures at the indicated times, and Tr activity was determined with the synthetic substrate *N*-carbobenzyloxy-Gly-Pro-Arg-*p*-nitroanilide. Activity was expressed as the percentage of the potential total activity, as determined on a wild-type Tg sample activated with enterokinase. Although not shown, control samples containing bovine serum albumin exhibited essentially identical autoactivation as samples with K15Q/R117H-Tg. Note that under the three conditions studied the time courses (*x* axis) were varied and the development of Tr activity (*y* axis) showed marked differences.

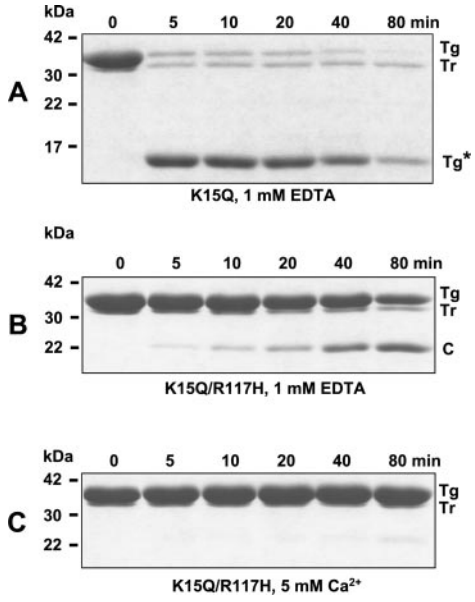

FIG. 7. **Trypsinolytic degradation of K15Q-Tg and K15Q/R117H-Tg.** Aliquots (5 μM, final concentration) of K15Q-Tg (*A*) or K15Q/R117H-Tg (*B*, *C*) were digested with 0.5 μM cationic Tr (final concentration) at 37 °C, in 0.1 M Tris-HCl (pH 8.0) and 1 mM K-EDTA (*A*, *B*) or 5 mM $CaCl_2$ (*C*). For comparison, see also digestion of K15Q-Tg in 5 mM Ca^{2+} in Fig. 5. Reactions were terminated at the indicated times by trichloroacetic acid precipitation and analyzed by reducing SDS-PAGE and Coomassie Blue staining. *Band C* is a unique proteolytic fragment observed only in the K15Q/R117H-Tg reactions. In the *0 min* samples trichloroacetic acid was added before Tg and Tr.

or K15Q-Tg*, K15Q/R117H-Tg was added to Tg at the same concentration. Although not shown, additional control samples, in which K15Q/R117H-Tg was replaced with bovine serum albumin, exhibited essentially identical Tg autoactivation to samples with K15Q/R117H-Tg. This finding demonstrates that K15Q/R117H-Tg has no measurable effect on Tg activation. In contrast, K15Q-Tg* afforded significant inhibition of Tg autoactivation (Fig. 6), which was particularly prominent at pH 5.0 and at 8.0 in the absence of Ca^{2+}. K15Q-Tg was less effective at pH 5.0 or at pH 8.0 in 5 mM Ca^{2+}, indicating that, in mixtures of intact and cleaved forms of K15Q-Tg, mostly the cleaved form is responsible for the inhibitory action. Consistent with this interpretation is the observation that at pH 8.0 in the absence of Ca^{2+} K15Q-Tg was virtually as effective an inhibitor as K15Q-Tg*, because under these conditions the majority of K15Q-Tg was rapidly converted to K15Q-Tg*. Although data are not shown, Tr-catalyzed activation of 100 μM bovine chymotrypsinogen A was inhibited by 80 μM K15Q-Tg* (final concentrations) ~2-fold. These experiments were carried out at pH 5.0, where the K_m for chymotrypsinogen activation is >0.5 mM.[3] Because the chymotrypsinogen concentration was well below its K_m, using the $K_i = K_i(\text{app})/(1 + S/K_m)$ equation (see Ref. 31 for further explanation), we could estimate an inhibitory constant (K_i) around 80 μM.

High Tr to Tg Ratio Results in Zymogen Degradation—Our observations described here clearly demonstrate that cleavage of the Arg^{117}-Val^{118} peptide bond in human cationic Tg with low concentrations of Tr does not *per se* lead to rapid degradation of Tg. Instead, due to Tr-catalyzed re-synthesis, intact Tg is reconstituted, eventually resulting in a dynamic equilibrium between single-chain and two-chain forms of Tg.

This picture, however, is only true when the Tr to Tg ratio is relatively low (*e.g.* 1:160, see Fig. 4). When K15Q-Tg was digested in the absence of Ca^{2+} with a higher (1:10) ratio of Tr, not only cleavage after Arg^{117} occurred, but overall degradation of Tg and Tg* was also readily apparent (Fig. 7*A*). The intensity of both the Tg and Tg* bands decreased over time, without yielding any detectable cleavage products. Surprisingly, similar experiments on K15Q-Tg carrying the Arg^{117} → His mutation (K15Q/R117H-Tg) also indicated significant degradation (Fig. 7*B*), but in this case a single major proteolytic fragment (*band C* in Fig. 7*B*) was detected. Protein sequencing revealed only the original Tg N terminus, indicating that *band C* contains only the N-terminal cleavage product. On the basis of the apparent molecular weight of the product, the cleavage site was placed in the C-terminal half of Tg and was tentatively identified as the Lys^{188}-Asp^{189} peptide bond. Autocatalytic cleavage at the same site was also described in rat anionic Tg (16), and bovine Tr (32), where it was shown to inactivate the enzyme. Note that digestion of the Lys^{188}-Asp^{189} bond in all likelihood also takes place in K15Q-Tg, but due to simultaneous cleavage after Arg^{117} the fragments generated would be too small to detect on the routinely used 12% gels. Finally, 5 mM Ca^{2+} completely stabilized both K15Q-Tg (see Fig. 5) and K15Q/

[3] M. Sahin-Tóth, unpublished observations.

R117H-Tg (Fig. 7*C*), because no degradation was evident on gels.

To assess the effect of the R117H mutation on Tg degradation, we compared degradation kinetics of K15Q-Tg and K15Q/R117H-Tg. In our definition, Tg degradation was represented by the disappearance of those K15Q-Tg forms, which in a wild-type background could be potentially activated to Tr. Consequently, conversion of K15Q-Tg to K15Q-Tg* cannot be viewed as degradation, because wild-type Tg* can be activated to fully active Tr*. In contrast, cleavage at Lys^{188} (*i.e. band C* in Fig. 7*B*) can be regarded as a real degradation step, because this results in a Tg species that cannot give rise to active Tr. Therefore, in Fig. 7*A* the decrease in the sum of the density of bands Tg and Tg* was measured, whereas in Fig. 7*B* the disappearance of the intact Tg band was quantitated. The calculated rates of degradation for K15Q-Tg and K15Q/R117H-Tg were measurably different (39 nM Tg/min and 22 nM Tg/min, respectively), indicating an almost 2-fold stabilizing effect of the R117H mutation. Protein sequencing demonstrated that both chains of Tg* (Fig. 7*A*) were degraded at similar rates, because the ratio of the N- and C-terminal fragments in the Tg* band remained 1:1 over the time course. In contrast, *band C* generated from K15Q/R117H-Tg was stable, indicating that the R117H mutation protects the trypsinolytic sites in the N-terminal half of the protein and "re-directs" autolysis to the Lys^{188}-Asp^{189} bond. Similar observations were also reported with rat anionic Tr (15) and Tg (16, 17).

Finally, it is interesting to compare the rate of cleavage at Arg^{117} and at other trypsinolytic sites. As judged from Fig. 4, in the absence of Ca^{2+} at a 1:160 Tr to Tg ratio it takes about 0.5 min to convert half of K15Q-Tg to K15Q-Tg*. At the same Ca^{2+} concentration, but at a 16-fold higher 1:10 Tr to Tg ratio, the $t_{½}$ for the overall trypsinolytic degradation of K15Q-Tg (Fig. 7*A*) is ~60 min. Therefore, in the absence of Ca^{2+}, Arg^{117} is almost *2000-fold* ($16 \times 60/0.5 = 1920$) more accessible for proteolysis than any other tryptic cleavage site in Tg.

DISCUSSION

Autocatalytic cleavage at Arg^{117} was first described more than 30 years ago in preparations of bovine cationic Tr (28), and it has been documented in porcine (29), rat (16–18, 33), and human (19, 34) Tr or Tg since then. More recently, mutagenesis studies on rat Tr indicated that the R117N replacement stabilized against autocatalytic inactivation (15) and led to the conclusion that Arg^{117} plays a fundamental role in the degradation of Tr. It was argued that cleavage of the Arg^{117}-Val^{118} bond, which is located on a surface loop separating the two globular domains of Tr, destabilizes the loop and leads to rapid and extensive proteolysis at multiple cleavage sites. On the basis of these observations, trypsinolytic cleavage at Arg^{117} has been viewed as the first step of a degradation pathway in human cationic Tr and Tg, which can curb the development of premature Tr activity in the pancreas (2, 35).

The observations presented in this paper redefine the role of Arg^{117}. In stark contrast to current dogma, proteolysis of the Arg^{117}-Val^{118} bond was not followed by rapid Tg degradation. Instead, re-synthesis of the peptide bond was observed, and eventually an equilibrium was attained between Tg and Tg*. The hydrolysis equilibrium was Ca^{2+}-dependent, and K_{hyd} varied from 5.4 in 1 mM EDTA (~15% intact Tg) to 0.7 in 5 mM Ca^{2+} (~60% intact Tg). Changes in K_{hyd} were at least partly due to the altered reactivity of Arg^{117}, as the *rate* of cleavage was diminished by increasing Ca^{2+} concentrations, and a difference of at least 20-fold was observed in 1 mM EDTA *versus* 5 mM Ca^{2+}. Protease-mediated peptide bond synthesis is a rare occurrence under physiological conditions due to the enthalpic and entropic barriers that render the reverse proteolytic condensation of peptides thermodynamically unfavorable. Shifting the peptide-bond hydrolysis equilibrium toward synthesis usually requires the presence of organic co-solvents (36) or "molecular trapping" of the products (37). We have not found any example in the literature where under physiological conditions a peptide bond in a natural protein was so rapidly cleaved and re-synthesized as Arg^{117}-Val^{118}. One well-known example of tryptic synthesis is the reactive site bond in the standard mechanism, canonical Tr inhibitors (Ref. 24, and references therein). A common feature of these inhibitors is the presence of a hyper-exposed Arg or Lys residue on a rigid surface loop, which fits into the specificity pocket of Tr. The reactive site bond is then hydrolyzed at very *slow* rates until an equilibrium is reached between the modified (*i.e.* cleaved) and virgin (intact) inhibitors. Importantly, the same equilibrium can be demonstrated starting from cleaved inhibitors. The behavior of the Arg^{117}-Val^{118} bond in many respects is highly analogous to the reactive site bonds of canonical Tr inhibitors. Thus, Arg^{117} is hyper-exposed on a surface loop, cleavage at the Arg^{117}-Val^{118} bond results in an equilibrium between cleaved and intact Tg, and the same equilibrium is reached starting from cleaved Tg.

However, there are some interesting differences, too. In canonical Tr inhibitors the reactive loop is usually very rigid, in most cases stabilized by disulfide bonds in the vicinity of the scissile peptide bond. As a consequence of this characteristic stability, the structure of the reactive loop is usually identical in free inhibitors and in their complexes with Tr, exhibiting similar Ramachandran angles (24, 38). In contrast, there is no disulfide bond that would stabilize the loop containing Arg^{117} in Tg. This loop has a relatively high temperature factor in the mammalian Tg or Tr crystal structures, indicating significant flexibility. The Ramachandran angles of Arg^{117} and its neighboring residues in the human cationic trypsin crystal structure (34) are different from the "consensus" angles (38) of the reactive loop in canonical trypsin inhibitors. Another striking difference is the very high rate of cleavage of the Arg^{117}-Val^{118} bond, which is several orders of magnitude faster than proteolysis of reactive bonds in inhibitors. It remains an exciting question: Given the flexibility of Arg^{117} and the fast cleavage at this site, what structural determinants cause the unexpected re-synthesis of this bond? In any event, taken together the observations suggest that the Arg^{117}-Val^{118} bond is the reactive site of an inhibitory domain in Tg, which should have relatively low affinity to Tr. To examine this possibility, qualitative experiments were performed where autoactivation of cationic Tg was followed in the presence of 80 μM (final concentration) K15Q-Tg or K15Q-Tg*. Relative to control samples containing 80 μM K15Q/R117H-Tg, K15Q-Tg* significantly decreased the rate of autoactivation. Furthermore, by assessing the ability of K15Q-Tg* to inhibit the activation of bovine chymotrypsinogen a K_i of ~80 μM was estimated.

Can such a weak inhibitory action play a role in pancreatic physiology? Total Tg concentrations in human pancreatic juice were reported in the range of 4–40 μM (39). At this concentration the significance of Arg^{117}-mediated inhibition is questionable. However, inside the acinar cells, in the zymogen granules in particular, Tg concentrations can reach 1 mM or higher (estimated from Refs. 39, 40). At millimolar zymogen concentrations the contribution of the inhibitory domain of cationic Tg to zymogen stability can be significant.

Arguably, one of the remarkable conclusions of this study is that conversion of Tg to Tg* by cleavage of the Arg^{117}-Val^{118} bond is not the initial step of a degradation pathway, because no further cleavages in Tg or Tg* were observed with Tr concentrations that readily proteolyze Tg after Arg^{117}. However, experiments using high Tr concentrations revealed time-de-

pendent Tg breakdown, although at a rate that was almost 2000-fold slower than cleavage at Arg^{117}. Significant Tg degradation was observed only in the absence of Ca^{2+} at pH 8.0, whereas 5 mM Ca^{2+} completely stabilized K15Q-Tg (compare Figs. 5 and 7*A*). Mutation R117H decreased degradation of K15Q-Tg by almost 50%, apparently by protecting trypsinolytic sites in the N-terminal half of Tg. Thus, in K15Q/R117H-Tg only a single site in the C-terminal half of the protein (tentatively identified as the Lys^{188}-Asp^{189} bond) was cleaved to any significant extent. Interestingly, the R117H mutation did not seem to alter the stabilizing effect of Ca^{2+}, which afforded complete protection against degradation of K15Q/R117H-Tg (see Fig. 7*C*).

When taken as a whole, these observations offer novel insight into the complexity of possible failsafe mechanisms that protect against premature Tg activation in the pancreas. In case of unwanted zymogen activation, the first line of defense is PSTI, which can absorb up to 20% of the potential Tg activity (41). Once this pathway is saturated, at low Tr concentrations most of the cationic Tg is converted to Tg*, which inhibits further Tg activation. If Tg activation progresses and higher Tr concentrations appear, autocatalytic Tg breakdown becomes significant, which limits further Tg activation. In addition, autolysis of Tr might be a protective factor at higher Tr concentrations. Mutation R117H seems to lead to excessive Tr activity in the pancreas by interfering with multiple protective mechanisms. (i) The resistance of R117H Tr against autolysis is increased (20, 21). (ii) The mutation increases the spontaneous autoactivation of Tg (20, 21). Enhanced autoactivation cannot be explained by the increased autolytic resistance of R117H-Tr, because it is also observed under conditions where Tr autolysis is insignificant. (iii) The R117H mutant Tg cannot be converted to Tg*, and thus the inhibitory effect of Arg^{117} is lost. (iv) The R117H mutation stabilizes Tg against degradation by Tr.

Acknowledgments—Special thanks to Ron Kaback and Yonglin Hu for help with this project. Protein sequencing was carried out by David W. McCourt at Midwest Analytical, Inc., St. Louis, MO.

REFERENCES

1. Applebaum-Shapiro, S. E., Finch, R., Pfützer, R. H., Hepp, L. A., Gates, L., Amann, S., Martin, S., Ulrich, C. D., II, and Whitcomb, D. C. (2001) *Pancreatology* **1,** 439–443
2. Whitcomb, D. C., Gorry, M. C., Preston, R. A., Furey, W., Sossenheimer, M. J., Ulrich, C. D., Martin, S. P., Gates, L. K., Jr., Amann, S. T., Toskes, P. P., Liddle, R., McGrath, K., Uomo, G., Post, J. C., and Ehrlich, G. D. (1996) *Nat. Genet.* **14,** 141–145
3. Simon, P., Weiss, U. F., Sahin-Tóth, M., Perry, M., Nayler, O., Lenfers, B., Schnekenburger, J., Mayerle, J., Domschke, W., and Lerch, M. M. (2001) *J. Biol. Chem.*, in press
4. Le Marechal, C., Chen, J. M., Quere, I., Raguenes, O., Ferec, C., and Auroux, J. (2001) *BMC Genet.* **2,** 19
5. Pfützer, R., Myers, E., Applebaum-Shapiro, S., Finch, R., Ellis, I., Neoptolemos, J., Kant, J. A., and Whitcomb, D. C. (2002) *Gut* **50,** 271–272
6. Gorry, M. C., Gabbaizedeh, D., Furey, W., Gates, L. K., Jr, Preston, R. A., Aston, C. E., Zhang, Y., Ulrich, C., Ehrlich, G. D. and Whitcomb, D. C. (1997) *Gastroenterology* **113,** 1063–1068
7. Teich, N., Mossner, J., and Keim, V. (1998) *Hum. Mutat.* **12,** 39–43
8. Ferec, C., Raguenes, O., Salomon, R., Roche, C., Bernard, J. P., Guillot, M., Quere, I., Faure, C., Mercier, B., Audrezet, M. P., Guillausseau, P. J., Dupont, C., Munnich, A., Bignon, J. D., and Le Bodic, L. (1999) *J. Med. Genet.* **36,** 228–232
9. Witt, H., Luck, W., and Becker M. (1999) *Gastroenterology* **117,** 7–10
10. Chen, J. M., Raguenes, O., Ferec, C., Deprez, P. H., Verellen-Dumoulin, C., and Andriulli, A. (1999) *Gastroenterology* **117,** 1508–1509
11. Pfützer, R. H., and Whitcomb, D. C. (1999) *Gastroenterology* **117,** 1507–1508
12. Teich, N., Ockenga, J., Hoffmeister, A., Manns, M., Mössner, J., and Keim, V. (2000) *Gastroenterology* **119,** 461–465
13. Chen, J. M., Piepoli Bis, A., Le Bodic, L., Ruszniewski, P., Robaszkiewicz, M., Deprez, P. H., Raguenes, O., Quere, I., Andriulli, A., and Ferec, C. (2001) *Clin. Genet.* **59,** 189–193
14. Le Maréchal, C., Bretagne, J.-F., Raguénès, O., Quéré, I., Chen, J.-M., and Ferec, C. (2001) *Mol. Genet. Metab.* **74,** 342–344
15. Várallyai, É., Pál, G., Patthy, A., Szilágyi, L., and Gráf, L. (1998) *Biochem. Biophys. Res. Commun.* **243,** 56–60
16. Sahin-Tóth, M. (1999) *J. Biol. Chem.* **274,** 29699–29704
17. Sahin-Tóth, M., Gráf, L., and Tóth, M. (1999) *Biochem. Biophys. Res. Commun.* **264,** 505–508
18. Sahin-Tóth, M., and Tóth, M. (2000) *Biochem. Biophys. Res. Commun.* **275,** 668–671
19. Sahin-Tóth, M. (2000) *J. Biol. Chem.* **275,** 22750–22755
20. Sahin-Tóth, M., and Tóth, M. (2000) *Biochem. Biophys. Res. Commun.* **278,** 286–289
21. Sahin-Tóth, M. (2001) *Pancreatology* **1,** 461–465
22. Szilágyi, L., Kénesi, E., Katona, G., Kaslik, G., Juhász, G., and Gráf, L. (2001) *J. Biol. Chem.* **276,** 24574–24580
23. Halangk, M. W., Lerch, M. M., Brandt-Nedelev, B., Roth, W., Ruthenbuerger, M., Reinheckel, T., Domschke, W., Lippert, H., Peters, C., and Deussing, J. (2000) *J. Clin. Invest.* **106,** 773–781
24. Laskowski, M., Jr., and Qasim, M. A. (2000) *Biochim. Biophys. Acta* **1477,** 324–337
25. Chen, J. M., Ferec, C., Pfützer, R. H., and Whitcomb, D. C. (2000) *Gastroenterology* **119,** 277–279
26. Higaki, J. N., and Light, A. (1985) *Anal. Biochem.* **148,** 111–120
27. Kumazaki, T., and Ishii, S.-I. (1979) *J. Biochem.* **85,** 581–590
28. Maroux, S., and Desnuelle, P. (1969) *Biochim. Biophys. Acta* **181,** 59–72
29. Ru, B. G., Du, J. Z., Zeng, Y. H., Chen, L. S., Ni, Y. S., Tan, G. H., and Zhang, L. X. (1980) *Sci. Sin.* **23,** 1453–1460
30. Estell, D. A., and Laskowski, M., Jr. (1980) *Biochemistry* **19,** 124–131
31. Cheng, Y., and Prusoff, W. H. (1973) *Biochem. Pharmacol.* **22,** 3099–3108
32. Smith, R. L., and Shaw, E. (1969) *J. Biol. Chem.* **244,** 4704–4712
33. Kaslik, G., Patthy, A., Bálint, M., and Gráf, L. (1995) *FEBS Lett.* **370,** 179–183
34. Gaboriaud, C., Serre, L., Guy-Crotte, O., Forest, E., and Fontecilla-Camps, J.-C. (1996) *J. Mol. Biol.* **259,** 995–1010
35. Chen, J. M., Montier, T., and Ferec, C. (2001) *Hum. Genet.* **109,** 245–252
36. Homandberg, G. A., Mattis, J. A., and Laskowski, M., Jr. (1978) *Biochemistry* **17,** 5220–5227
37. Homandberg, G. A., Komoriya, A., and Chaiken, I. M. (1982) *Biochemistry* **21,** 3385–3389
38. Bode, W., and Huber, R. (1992) *Eur. J. Biochem.* **204,** 433–451
39. Rinderknecht, H, Renner, I. G., and Carmack, C. (1979) *Gut* **20,** 886–891
40. Goncz, K. K., Behrsing, R., and Rothman, S. S. (1995) *Cell Tissue Res.* **280,** 519–530
41. Rinderknecht, H. (1986) *Dig. Dis. Sci.* **31,** 314–321